Inorg. Chem. **2003**, *42*, 7978–7989

Solid-State and Solution Properties of Cationic Lanthanide Complexes of a New Neutral Heptadentate N4O3 Tripodal Ligand

Florence Bravard,[†] Yann Bretonnière,[†] Raphaël Wietzke,[†] Christelle Gateau,[†] Marinella Mazzanti,*[,†] Pascale Delangle,[†] and Jacques Pécaut[‡]

Laboratoire de Reconnaissance Ionique and Laboratoire de Coordination et Chiralité, Département de Recherche Fondamentale sur la Matière Condensée, Service de Chimie Inorganique et Biologique (FRE 2600), CEA-Grenoble, 38054 Grenoble, Cedex 09, France

Received June 18, 2003

The synthesis of the potentially heptadentate ligand tris[6-((2-*N*,*N*-diethylcarbamoyl)pyridyl)methyl]amine, tpaam, containing three pyridinecarboxamide arms connected to a central nitrogen is described. Lanthanide complexes of this ligand are prepared and characterized. The crystallographic structure of the complexes of three lanthanide ions (La, Nd, Lu) is determined. The lanthanide(III) complexes of tpaam crystallize as monomeric species (in the presence of chloride or iodide counterions) in which the ligand tpaam acts as a N4O3 donor. The crystal structures presented here show that the Ln–O and Ln–$N_{pyridyl}$ distances in the complexes of tpaam are similar to those found for the tpaa complexes (H_3tpaa = α,α′,α″-nitrilotri(6-methyl-2-pyridinecarboxylic acid) despite the difference in charge. A lengthening of the Ln–N_{apical} distance is observed in the tpaam complexes compared to the tpa (tris-[(2-pyridyl)methyl]amine) complexes which is more marked for larger lanthanides than for smaller ones. The solution structures of the tpaam complexes were analyzed across the 4f series and compared to the solution structures of the lanthanide complexes of the tetradentate ligand tpa. Proton NMR studies are in agreement with the presence of C_{3v} symmetric solution species for both ligands. For the larger lanthanides, the cation moves away from the apical nitrogen compared to the position occupied in tpa complexes, whereas for the smaller lanthanides, the metal ion is located in a similar position for the two ligands. Quite surprisingly, the formation constant of the Eu(tpaam)-Cl_3 complex in D_2O at 298 K (log $\beta_{110} = 2.34(4)$) is very similar to the one reported for Eu(tpa)Cl_3 (log $\beta_{110} = 2.49(4)$ at 298 K in D_2O) indicating that the addition of three amide groups to the ligand tpa does not lead to any increase in stability of the lanthanide complexes of tpaam compared to those of tpa.

1. Introduction

In recent years a significant effort has been made to design organic polydentate ligands for the complexation of lanthanide ions.[1−3] These studies have been motivated by the numerous applications of lanthanide complexes in medicine, catalysis, and materials science. Medicinal applications, such as the use of Gd complexes as magnetic resonance imaging (MRI) contrast agents, require very thermodynamically stable and/or kinetically inert complexes to avoid toxicity.[4,5] Anionic polyaminocarboxylate or polyaminophosphonate ligands are most often employed to achieve high stability in physiological conditions because neutral ligands tend to release lanthanide ions in these conditions. The development of lanthanide complexes that are stable with respect to ligand dissociation in physiological conditions is also of interest for the design of Ln(III) complexes active in catalyzing RNA cleavage in vivo.[6,7] Complexes of anionic polyaminocarboxylates are not active catalysts of RNA cleavage because of the reduced reactivity of the cation. To maintain the Lewis acid character of the free lanthanide ion responsible for the

* Author to whom correspondence should be addressed. E-mail: mazzanti@drfmc.ceng.cea.fr.
[†] Laboratoire de Reconnaissance Ionique.
[‡] Laboratoire de Coordination et Chiralité.

(1) Alexander, V. *Chem. Rev.* **1995**, *95*, 273.
(2) Piguet, C.; Bünzli, J.-C. G. *Chem. Soc. Rev.* **1999**, *28*, 347.
(3) Parker, D.; Dickins, R. S.; Puschmann, H.; Crossland, C.; Howard, J. A. K. *Chem. Rev.* **2002**, *102*, 1977.
(4) Caravan, P.; Ellison, J. J.; McMurry, T. J.; Lauffer, R. B. *Chem. Rev.* **1999**, *99*, 2293.
(5) Merbach, A. E.; Toth, E. *The Chemistry of Contrast Agents in Medical Magnetic Resonance Imaging*; Wiley: Chichester, U.K., 2001.
(6) Komiyama, M.; Takeda, N.; Shigekawa, H. *Chem. Commun.* **1999**, 1443.
(7) Morrow, J. R.; Buttrey, L. A.; Shelton, V. M.; Berback, K. *J. Am. Chem. Soc.* **1992**, *114*, 1903.

10.1021/ic034692e CCC: $25.00
Published on Web 10/28/2003

Chart 1

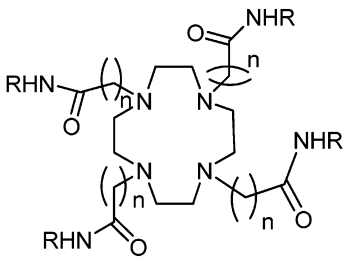

R=H , n=1 dotam
R= H , n=2 tcec
R=Me, n=1 dtma

catalytic activity, it is necessary to design neutral ligands leading to reasonably stable cationic complexes. Furthermore, the ligand should lead to complexes with coordination sites available for the direct binding of the substrate. The design of tripositive lanthanide complexes coordinatively unsaturated and resistant toward metal release in physiological conditions represents a real challenge, and only a few such complexes have been described.[8]

Tripositive lanthanide complexes of tetraamide ligands derived from 1,4,7,10-tetraazacyclododecane as well as Ln(III) complexes of hexadentate Schiff-base macrocycles have been shown to be kinetically stable with respect to ligand dissociation in water and to catalyze RNA cleavage (see Chart 1).[7,9−12] The neutral octadentate ligand dotam (where dotam = 1,4,7,10-tetrakis-(carbamoylmethyl)-1,4,7,10-tetrazacyclododecane) yields a 10-coordinate lanthanum complex that is inert toward ligand dissociation in water.[11] Although an important loss in complex stability has been observed for the tripositive Gd(III) complex of the tetramide dtma (log K = 12.8(1))[13] with respect to the Gd(III) complex of dota (log K = 24.67(7)) (where dtma = 1,4,7,10-tetrakis-(methylcarbamoylmethyl)-1,4,7,10-tetrazacyclododecane and H_4dota = 1,4,7,10-tetraazacyclododecane-*N*,*N*′,*N*″,*N*‴-tetraacetic acid), a large contribution by the amide group to the complex stability is suggested by the observed complete dissociation in water of the similar complex $Gd(tcec)^{3+}$ (where tcec = 1,4,7,10-tetrakis-(carbamoylethyl)-1,4,7,10-tetrazacyclododecane) in which the pendant amide groups are less tightly bound.[14] The magnitude of the contribution of the amide functional groups to the stability of Gd(III) complexes of dtpa (where H_5dtpa = diethylenetriaminepentaacetic acid) derivatives has been studied by Paul-Roth and Raymond who estimated it to be 3.38 log units for each amide group.[15] The replacement of benzimidazole groups by carboxamide binding units has also been reported to lead to an increased resistance toward ligand dissociation of self-assembled dinuclear lanthanide helicates.[16] Moreover, the nine-coordinate complexes of a nonadentate covalent tripode containing pyridine-2,6-dicarboxamide binding units were described as showing good resistance to ligand dissociation (log β = 5−7.5 in 95:5 acetonitrile/water), although there are no data available about their stability in pure water.[17]

We have previously studied the complexation of lanthanide(III) ions by the neutral tripodal tetradentate ligand tpa (tris[(2-pyridyl)methyl]amine).[18] Lanthanide complexes of tpa dissociate partially in water (log $K \sim 2$). More recently, we have described the new trianionic heptadentate tripodal ligand tpaa (H_3tpaa = α,α′,α″-nitrilotri(6-methyl-2-pyridinecarboxylic acid)) containing three pyridinecarboxylate arms connected to a nitrogen atom leading to the MRI-relevant nonadentate gadolinium complex $[Gd(tpaa)(H_2O)]_2$ with improved relaxation efficiency. This neutral complex has a reasonable physiological stability with a pGd = 11.2 for Gd(III) ($-\log[M]_{free}$ at pH 7.4; $[M]_{total}$ = 1 μM and $[tpaa]_{total}$ = 10 μM).[19,20] To investigate if the addition of coordinating amide groups to the tetradentate tpa ligand would yield tripositive Ln(III) complexes with an increased stability toward ligand dissociation in water, we have synthesized the new neutral heptadentate ligand tpaam (tris[6-((2-*N*,*N*-diethylcarbamoyl)pyridyl)methyl]amine). (For representations of tpa, H_3tpaa, and tpaam see Chart 2.) This ligand will also allow us to evaluate the effect of replacement of the carboxylate coordinating groups with coordinating amide oxygens in these tripodal systems. Here we report the solid-state and solution properties of Ln(III) complexes of tpaam, and we compare them with those of the tpa and tpaa complexes. Unexpectedly, the formation constant of the Eu(III) tpaam complex in water was found to be very similar to that of the tpa complex, despite the presence of three additional coordinating amide groups.

2. Experimental Section

2.1. General Information. ^{1}H and ^{13}C NMR spectra were recorded on Varian Mercury 400 and Bruker 200 spectrometers. NMR chemical shifts are reported in ppm with solvent as internal reference. Mass spectra were obtained with a LCQ ion trap (Finnigan-Thermoquest) equipped with an electrospray source. Microanalyses were performed by the Service Central d'Analyses (Vernaison-69). Elemental analysis of the $[Lu(tpaam)I_3]$ complex was performed under argon by Analytische Laboratorien GMBH at Lindlar, Germany. Solvents and starting materials were obtained from commercial suppliers and were used as received. 6-Diethylcarbamoyl-pyridine-2-carboxylic acid methyl ester was synthesized

(8) Oh, S. J.; Choi, Y.-S.; Hwangbo, S.; Bae, C. S. *Chem. Commun.* **1998**, 2189.
(9) Dickins, R. S.; Howard, J. A. K.; Lehmann, C. W.; Moloney, J.; Parker, D.; Peacock, R. D. *Angew. Chem., Int. Ed. Engl.* **1997**, *36*, 521.
(10) Aime, S.; Barge, A.; Bruce, I. J.; Botta, M.; Howard, J. A. K.; Moloney, J.; Parker, D.; de Sousa, A. S.; Woods, M. *J. Am. Chem. Soc.* **1999**, *121*, 5762.
(11) Amin, S.; Morrow, J. R.; Lake, C. H.; Churchill, M. R. *Angew. Chem., Int. Ed. Engl.* **1994**, *33*, 773.
(12) Parker, D.; Williams, J. A. G. *J. Chem. Soc., Perkin Trans. 2* **1995**, 1305.
(13) Bianchi, A.; Calabi, L.; Giorgi, C.; Losi, P.; Mariani, P.; Paoli, P.; Rossi, P.; Valtancoli, B.; Virtuani, M. *J. Chem. Soc., Dalton Trans.* **2000**, 697.
(14) Morrow, J. R.; Amin, S.; Lake, C. H.; Churchill, M. R. *Inorg. Chem.* **1993**, *32*, 4566.
(15) Paul-Roth, C.; Raymond, K. N. *Inorg. Chem.* **1995**, *34*, 1408.
(16) Martin, N.; Bünzli, J.-C.; McKee, V.; Piguet, C.; Hopfgartner, G. *Inorg. Chem.* **1998**, *37*, 577.
(17) Renaud, F.; Piguet, C.; Bernardinelli, G.; Bünzli, J.-C. G.; Hopfgartner, G. *J. Am. Chem. Soc.* **1999**, *121*, 9326.
(18) Wietzke, R.; Mazzanti, M.; Latour, J.-M.; Pecaut, J.; Cordier, P.-Y.; Madic, C. *Inorg. Chem.* **1998**, *37*, 6690.
(19) Bretonnière, Y.; Mazzanti, M.; Dunand, F. A.; Merbach, A. E.; Pécaut, J. *Chem. Commun.* **2001**, 621.
(20) Bretonnière, Y.; Mazzanti, M.; Dunand, F. A.; Merbach, A. E.; Pécaut, J. *Inorg. Chem.* **2001**, *40*, 6737.

Chart 2

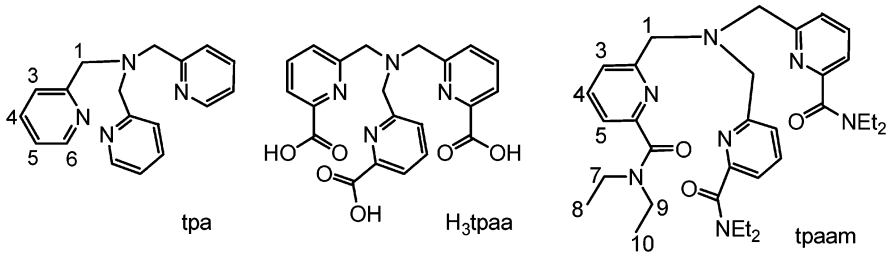

according to the procedure of Chauvin et al.[21] The synthesis of the ligand tpaam was carried out under an atmosphere of argon. Catalytic hydrogenation was performed within a TOP 80 reactor with controlled hydrogen pressure, temperature, and rotation speed. Flash chromatography was performed using silica gel Si60 (40−63 μm, Merck). Preparative high-performance liquid chromatography (HPLC) was performed with a Septech GP-900 controller equipped with a Dynamax absorbance detector ($\lambda = 260$ nm). The column used was a Purosphere RP-18 column (10 μm, 20 × 5 cm) run at 60 mL/min. The preparation of the lanthanide complexes of tpaam from the $[LnI_3(THF)_x]$ salts (THF = tetrahydrofuran) was performed in rigorously anhydrous conditions in a glovebox (<1 ppm water). The complexes $[LnI_3(THF)_x]$ (Ln = La, $x = 4$; Ln = Lu, $x = 3.5$) were prepared by stirring anhydrous lanthanide iodides (purchased from Aldrich) in THF overnight. The white powder obtained after filtration was purified by extraction in hot THF.

2.2. Synthesis of the Ligand tpaam. 2.2.1. *N*,*N*-Diethyl(6-hydroxymethyl)pyridine-2-carboxamide (2). 6-Diethylcarbamoylpyridine-2-carboxylic acid methyl ester (**1**) (0.556 g, 2.35 mmol) was dissolved in dry MeOH (10 mL). $NaBH_4$ (0.249 g, 6.59 mmol) was added in small portions, and the reaction mixture was refluxed for 4 h until all of the starting material had been consumed and thin-layer chromatography (TLC) was consistent with one major product. After the mixture had cooled to room temperature, the reaction was stopped by adding water (50 mL). The aqueous layer was extracted with CH_2Cl_2 (4 × 50 mL). The organic layer was dried with Na_2SO_4 and evaporated to dryness affording a light yellow residue. The residue was purified by flash chromatography (20 g silica gel, CH_2Cl_2/MeOH gradient from 100/0 to 90/10 (v/v)) yielding a white solid (0.348 g, 71%).

^{1}H NMR (400 MHz, $CDCl_3$, δ): 1.24 (t, $J = 7.0$ Hz, 3H, NCH_2CH_3), 1.31 (t, $J = 7.0$ Hz, 3H, NCH_2CH_3), 3.35 (q, $J = 7.0$ Hz, 2H, NCH_2CH_3), 3.60 (q, $J = 7.0$ Hz, 2H, NCH_2CH_3), 3.68 (s_{broad}, 1H, CH_2OH), 4.83 (s, 2H, CH_2OH), 7.35 (d, $J = 7.7$ Hz, 1H, H^3/H^5), 7.51 (d, $J = 7.7$ Hz, 1H, H^3/H^5), 7.85 (t, $J = 7.7$ Hz, 1H, H^4). ^{13}C NMR (100 MHz, $CDCl_3$, δ): 13.02 (NCH_2CH_3), 14.56 (NCH_2CH_3), 40.30 (NCH_2CH_3), 43.41 (NCH_2CH_3), 64.24 (CH_2-OH), 121.11 (CH_{Ar}), 121.66 (CH_{Ar}), 138.03 (CH_{Ar}), 153.96 (C_{Ar}), 158.61 (C_{Ar}), 168.36 (C=O). ES-MS (*m*/*z*): 209.1 $[M + H]^+$.

2.2.2. *N*,*N*-Diethyl(6-bromomethyl)pyridine-2-carboxamide (3b). *N*,*N*-Diethyl(6-hydroxymethyl)pyridine-2-carboxamide (1.00 g, 4.80 mmol) was dissolved in dry CH_2Cl_2 (30 mL), and the mixture was cooled to 0 °C. Then a solution of thionyl bromide (0.93 mL, 12.00 mmol) in dry CH_2Cl_2 (80 mL) was added dropwise. The reaction mixture was stirred overnight at room temperature and then poured into 150 mL of iced water. The organic layer was separated, and the aqueous layer was extracted with CH_2Cl_2 (3 × 75 mL). The combined organic layers were washed with 1 M aqueous $NaHCO_3$ solution (2 × 100 mL), dried with Na_2SO_4, and evaporated. The crude residue (1.29 g, 99%) was isolated as a light pink oil and used without further purification.

^{1}H NMR (400 MHz, $CDCl_3$, δ): 1.24 (t, $J = 7.0$ Hz, 3H, NCH_2CH_3), 1.29 (t, $J = 7.0$ Hz, 3H, NCH_2CH_3), 3.39 (q, $J = 7.0$ Hz, 2H, NCH_2CH_3), 3.57 (q, $J = 7.0$ Hz, 2H, NCH_2CH_3), 4.55 (s, 2H, CH_2Br), 7.45 (d, $J = 7.8$ Hz, 1H, H^3/H^5), 7.52 (d, $J = 7.8$ Hz, 1H, H^3/H^5), 7.77 (t, $J = 7.8$ Hz, 1H, H^4). ^{13}C NMR (100 MHz, $CDCl_3$, δ): 13.05 (NCH_2CH_3), 14.58 (NCH_2CH_3), 33.61 (CH_2Br), 40.64 (NCH_2CH_3), 43.65 (NCH_2CH_3), 122.70 (CH_{Ar}), 123.99 (CH_{Ar}), 138.23 (CH_{Ar}), 155.03 (C_{Ar}), 155.70 (C_{Ar}), 168.12 (C=O). ES-MS (*m*/*z*): 271.0/273.0 (100/97) $[M + H]^+$.

2.2.3. *N*,*N*-Diethyl(6-azidomethyl)pyridine-2-carboxamide (4). Methanesulfonyl chloride (0.45 mL, 5.76 mmol) was added to a cold (0 °C) mixture of *N*,*N*-diethyl(6-hydroxymethyl)pyridine-2-carboxamide (1.20 g, 5.76 mmol) and triethylamine (0.81 mL, 5.76 mmol) in dry toluene (40 mL). The resulting mixture was stirred for 1 h and the temperature was allowed to rise from 0 °C to room temperature. Then sodium azide (3.00 g, 46.09 mmol), tetrabutylammonium bromide (0.204 g, 0.63 mmol), and H_2O (12 mL) were added. The reaction mixture was stirred overnight at 90 °C. After the mixture had cooled to room temperature, the organic layer was separated from the mixture and the aqueous layer was extracted with toluene (3 × 50 mL). The combined organic layers were dried with Na_2SO_4 and evaporated. The crude residue (1.31 g, 97%) was isolated as a colorless oil and used without further purification.

^{1}H NMR (400 MHz, $CDCl_3$, δ): 1.22 (t, $J = 7.0$ Hz, 3H, NCH_2CH_3), 1.29 (t, $J = 7.0$ Hz, 3H, NCH_2CH_3), 3.39 (q, $J = 7.0$ Hz, 2H, NCH_2CH_3), 3.58 (q, $J = 7.0$ Hz, 2H, NCH_2CH_3), 4.50 (s, 2H, CH_2N_3), 7.38 (d, $J = 7.7$ Hz, 1H, H^3/H^5), 7.55 (d, $J = 7.7$ Hz, 1H, H^3/H^5), 7.81 (t, $J = 7.7$ Hz, 1H, H^4).

2.2.4. *N*,*N*-Diethyl(6-aminomethyl)pyridine-2-carboxamide (5). Crude *N*,*N*-diethyl(6-azidomethyl)pyridine-2-carboxamide (1.31 g, 5.60 mmol) was dissolved in MeOH (160 mL) and reduced under hydrogen pressure (1 bar) in the presence of 10% palladium/charcoal (0.152 g) for 4 days. Then the mixture was filtered through a pad of Celite to remove the catalyst and evaporated to dryness. The resulting crude product (1.08 g, 93%) was isolated as a colorless oil and used without further purification.

^{1}H NMR (400 MHz, $CDCl_3$, δ): 1.21 (t, $J = 7.0$ Hz, 3H, NCH_2CH_3), 1.29 (t, $J = 7.0$ Hz, 3H, NCH_2CH_3), 1.70 (s_{broad}, 2H, NH_2), 3.36 (q, $J = 7.0$ Hz, 2H, NCH_2CH_3), 3.56 (q, $J = 7.0$ Hz, 2H, NCH_2CH_3), 3.99 (s, 2H, CH_2NH_2), 7.29 (d, $J = 7.6$ Hz, 1H, H^3/H^5), 7.43 (d, $J = 7.6$ Hz, 1H, H3/H5), 7.72 (t, $J = 7.6$ Hz, 1H, H^4). ^{13}C NMR (100 MHz, $CDCl_3$, δ): 13.09 (NCH_2CH_3), 14.60 (NCH_2CH_3), 40.36 (NCH_2CH_3), 43.44 (NCH_2CH_3), 47.84 (CH_2-NH_2), 121.25 (CH_{Ar}), 121.77 (CH_{Ar}), 137.56 (CH_{Ar}), 154.94 (C_{Ar}), 160.96 (C_{Ar}), 168.91 (C=O). ES-MS (*m*/*z*): 208.1 $[M + H]^+$.

2.2.5. Tris[6-((2-*N*,*N*-diethylcarbamoyl)pyridyl)methyl]amine (tpaam). *N*,*N*-Diethyl(6-bromomethyl)pyridine-2-carboxamide (0.549 g, 2.03 mmol) and anhydrous K_2CO_3 (0.333 g, 2.41 mmol) were added to a solution of *N*-diethyl(6-aminomethyl)pyridine-2-carboxamide (0.200 g, 0.96 mmol) in dry CH_3CN (20 mL). The reaction mixture was refluxed for 24 h. After the mixture had cooled to room temperature, the solution was evaporated to dryness and the residue was dissolved in CH_2Cl_2 (100 mL). The organic layer

(21) Chauvin, A.-S.; Tripier, R.; Bünzli, J.-C. *Tetrahedron Lett.* **2001**, *42*, 3089.

was washed with 1 M aqueous $NaHCO_3$ solution (2 × 50 mL), dried with Na_2SO_4, and evaporated. The resulting crude product was purified by preparative HPLC with CH_3CN/H_2O (60/40 v/v) as eluant, yielding a colorless oil (0.447 g, 78%).

^{1}H NMR (400 MHz, $CDCl_3$, δ): 1.23 (t, J = 7.0 Hz, 3H, H^8/H^{10}), 1.29 (t, J = 7.0 Hz, 3H, H^8/H^{10}), 3.38 (q, J = 7.0 Hz, 2H, H^7/ H^9), 3.57 (q, J = 7.0 Hz, 2H, H^7/ H^9), 4.68 (s, 2H, H^1), 7.50 (d, J = 7.6 Hz, 1H, H^3/H^5), 7.52 (d, J = 7.6 Hz, 1H, H^3/H^5), 7.81 (t, J = 7.6 Hz, 1H, H^4). ^{13}C NMR (100 MHz, $CDCl_3$, δ): 13.07 (C^8/C^{10}), 14.53 (C^8/C^{10}), 40.42 (C^7/C^9), 43.47 (C^7/C^9), 60.28 (C^1), 121.67 (CH_{Ar}), 123.39 (CH_{Ar}), 137.49 (CH_{Ar}), 154.76 (C_{Ar}), 158.43 (C_{Ar}), 168.79 (C=O). ES-MS (m/z): 588.3 $[M + H]^+$. Anal. Calcd for $C_{33}H_{45}N_7O_3 \cdot 0.5H_2O$ (596.78): C, 66.42; H, 7.77; N, 16.43. Found: C, 66.79; H, 7.78; N, 16.34.

2.3. Preparation of the Complexes. 2.3.1. Ln(tpaam)X_3 (X = OTf (Triflate), Ln = Eu, Tb; X = ClO_4, Ln = La, Nd). Tpaam (0.3 mmol) was added to a solution of $LnX_3 \cdot H_2O$ (0.3 mmol) (X = ClO_4 (n = 6−7), OTf (n = 0), Ln = La, Nd, Eu, Tb) in acetonitrile (7 mL). The reaction mixture was stirred at room temperature for 1 h. The complexes Ln(tpaam)X_3 were obtained as beige solids in 70−80% yield by addition of diethyl ether.

^{1}H NMR (400 MHz, CD_3CN, 298 K, δ): La(tpaam)$(ClO_4)_3$, 8.09 (t, 1H, H^4), 7.76 (d, 1H, H^5), 7.66 (d, 1H, H^3), 4.27 (s, 2H, H^1), 3.66 (m, 4H, H^7, H^9), 1.40 (t, 3H, H^{10}), 1.11 (t, 3H, H^8); Nd(tpaam)$(ClO_4)_3$, 10.98 (s, 1H, H^5), 9.28 (s, 1H, H^4), 7.58 (s, 1H, H^3), 6.44 (s, 2H, H^7/H^9), 5.17 (s, 2H, H^7/H^9), 2.91 (s, 3H, H^8/H^{10}), 1.90 (s, 2H, H^1), 1.31 (s, 3H, H^8/H^{10}); Eu(tpaam)$(OTf)_3$, 6.78 (t, 1H, H^4), 6.63 (d, 1H, H^3), 4.26 (d, 1H, H^5), 2.26 (m, 2H, H^7/H^9), 1.44 (m, 2H, H^7/H^9), 1.11 (m, 5H, H^1, H^8/H^{10}), 0.15 (t, 3H, H^8/H^{10}). ES-MS (acetonitrile, m/z): La(tpaam)$(ClO_4)_3$, 923.7 [La(tpaam)$(ClO_4)_2]^+$, 412.5 [La(tpaam)$(ClO_4)]^{2+}$, 242.2 [La(tpaam)$]^{3+}$; Nd(tpaam)$(ClO_4)_3$, 929 [Nd(tpaam)$(ClO_4)_2]^+$, 415 [Nd(tpaam)$(ClO_4)]^{2+}$, 244 [Nd(tpaam)$]^{3+}$; Eu(tpaam)$(OTf)_3$, 1038 [Eu(tpaam)$(OTf)_2]^+$, 444.5 [Eu(tpaam)$(OTf)]^{2+}$; Tb(tpaam)$(OTf)_3$, 1044 [Tb(tpaam)$(OTf)_2]^+$, 447.7 [Tb(tpaam)$(OTf)]^{2+}$. Anal. Calcd for Eu(tpaam)$(OTf)_3$: C, 36.43; H, 3.82; N, 8.26. Found: C, 37.06; H, 4.09; N, 8.53. Anal. Calcd for Tb(tpaam)$(OTf)_3 \cdot 2.5H_2O$: C, 34.90; H, 4.07; N, 7.91. Found: C, 34.82; H, 3.93; N, 7.82. Anal. Calcd for La(tpaam)$(ClO_4)_3 \cdot 4H_2O$: C, 36.13; H, 4.87; N, 8.94. Found: C, 36.31; H, 4.67; N, 8.80. Anal. Calcd for Nd(tpaam)$(ClO_4)_3 \cdot 3H_2O$: C, 36.55; H, 4.74; N, 9.04. Found: C, 36.35; H, 4.56; N, 8.79.

2.3.2. Ln(tpaam)Cl_3. Tpaam (0.2 mmol) was added to a solution of $LnCl_3 \cdot nH_2O$ (n = 6−7, Ln = La, Eu, Tb, Lu) (0.2 mmol) in methanol (6 mL). The reaction mixture was stirred for 2 h and then evaporated (3 mL). After diethyl ether (25 mL) was added, the complexes Ln(tpaam)Cl_3 were isolated as cream solids in 50% yield.

X-ray quality crystals of the complex $\{[Nd(tpaam)(Cl)(Cl)_{0.5}(MeOH)_{0.5}]_2[Nd(Cl)_5(MeOH)]\}(Cl) \cdot 3MeOH$, **6**, were obtained by slow diffusion of diethyl ether into a 1:1 mixture of $NdCl_3 \cdot 7H_2O$ and tpaam in acetonitrile.

The elemental analyses of all of these complexes indicate the presence of cocrystallized $LnCl_3$, but a satisfactory analysis was obtained only for Eu probably because of the hygroscopic character of these compounds.

Anal. Calcd for $[Eu(tpaam)](EuCl_3)_{0.5} \cdot 1.5MeOH$: C, 40.40; H, 4.98; N, 9.58. Found: C, 39.69; H, 5.24; N, 9.86. ES-MS (methanol, m/z): La(tpaam)Cl_3, 795.8 [La(tpaam)$(Cl_2)]^+$, 380.6 [La(tpaam)$Cl]^{2+}$, 362.7 [La(tpaam) − H$]^{2+}$; Eu(tpaam)Cl_3, 809.8 [Eu(tpaam)$Cl_2]^+$, 387.5 [Eu(tpaam)$Cl]^{2+}$, 369.5 [Eu(tpaam) − H$]^{2+}$; Tb(tpaam)Cl_3, 815.9 [Tb(tpaam)$Cl_2]^+$, 390.5 [Tb(tpaam)$Cl]^{2+}$, 372.5 [Tb(tpaam) − H$]^{2+}$; Lu(tpaam)Cl_3, 831.9 [Lu(tpaam)$Cl_2]^+$, 398.6 [Lu(tpaam)$Cl]^{2+}$, 380.7 [Lu(tpaam) − H$]^{2+}$.

2.3.3. La(tpaam)I_3 and Lu(tpaam)I_3. Tpaam (10 mg, 0.017 mmol) was added to a solution of $LuI_3(THF)_{3.5}$ (14 mg, 0.018 mmol) in pyridine (1 mL). The reaction mixture was stirred for 10 min, and then n-hexane (1 mL) was allowed to slowly diffuse into the resulting yellow solution. After 24 h, the complex Lu(tpaam)I_3 was isolated as a white crystalline solid in 75% yield.

^{1}H NMR (200 MHz, CD_3CN, 298 K, δ): [Lu(tpaam)I_3], 8.24 (t, 1H, H^4), 7.94 (d, 1H, H^5), 7.84 (d, 1H, H^3), 4.57 (s, 2H, H^1), 3.71 (q, 2H, H^7), 3.82 (q, 2H, H^9), 1.46 (t, 3H, H^{10}), 1.31 (t, 3H, H^8). Anal. Calcd for [Lu(tpaam)]I_3: C, 34.67; H, 3.94; N, 8.58. Found: C, 34.46; H, 3.88; N, 8.99. X-ray quality crystals of the complexes $[La(tpaam)(I)_2]I \cdot 0.25py$ (**7**) and $[Lu(tpaam)I](I)_2 \cdot 0.25CH_3CN \cdot 0.5py$ (**8**) were obtained by slow diffusion of n-hexane into a 1:1 mixture of $LnI_3(THF)_4$ (Ln = La, Lu) and tpaam in 50/50 acetonitrile/pyridine.

^{1}H NMR (200 MHz, CD_3CN, 298 K, δ): La(tpaam)I_3, 8.07 (t, 1H, H^4), 7.73 (d, 1H, H^5), 7.66 (d, 1H, H^3), 4.38 (s, 2H, H^1), 3.64 (m, 4H, H^7, H^9), 1.42 (t, 3H, H^{10}), 1.30 (t, 3H, H^8).

2.4. Solution NMR Studies. For proton NMR studies the Ln(tpaam)Cl_3 complexes were prepared in situ by dissolving $LnCl_3 \cdot 6H_2O$ (4.2 μmol) in 700 μL of a stock solution of the ligand in methanol-d_4 (0.006 mol L^{-1}). Solutions of the Ln(tpa)Cl_3 complexes (0.01 mol L^{-1}) were prepared in a similar way. The samples were degassed by the freeze−pump−thaw technique. Longitudinal relaxation times were measured using a nonselective inversion−recovery pulse sequence. The T_1 values were obtained from a three-parameter fit of the data to an exponential recovery function.

2.5. Stability Constant Determination by NMR Spectroscopy. The samples used for the determination of the apparent stability constants were prepared by mixing appropriate volumes of stock solutions of the ligand (~0.01 mol L^{-1}) and of the europium chloride salt (~0.01 mol L^{-1}) in deuterium oxide at a fixed ionic strength (1 mol L^{-1} KCl). The ligand concentrations were determined by potentiometric titration and the metal concentrations by EDTA titrations using xylenol orange indicator. NMR spectra were recorded on either a UNITY or a MERCURY 400 Varian spectrometer with 10 s relaxation delays. The apparent affinity constants β_{110}^{app} were calculated from the free ligand and complex concentrations, determined by deconvolution of the ^{1}H NMR signals giving precise peak integral values. The obtained values were the results of three independent measurements (the use of different metal/ligand ratios did not affect the value of the stability constant). Because the ligands exist as a mixture of L and LH^+ at the sample pD (measured pD = 6.5−7), the stability constants β_{110} defined in eq I and the apparent constant β_{110}^{app} are related by eq II, where K_a is the first protonation constant of the ligand (the protonation constants of tpa were determined to be pK_{a1} = 5.98(3), pK_{a2} = 4.19(7), and pK_{a3} = 2.2(2), and the protonation constant of tpaam was determined to be pK_a = 4.88(3) (0.1 mol L^{-1} KCl, 298 K) by potentiometric titration). The calculated $\log(\beta_{110})$ values for europium (2.34(4) for tpaam and 2.49(4) for tpa) are not significantly different from the measured $\log(\beta_{110}^{app})$ values.

$$Eu^{3+} + L = [EuL]^{3+} \qquad \beta_{110} \tag{I}$$

$$\beta_{110} = \beta_{110}^{app}\left(1 + \frac{[H^+]}{K_a}\right) \tag{II}$$

2.6. X-ray Crystallography. All diffraction data were taken using a Bruker SMART charge coupled device (CCD) area detector three-circle diffractometer (Mo Kα radiation, graphite monochromator, λ = 0.710 73 Å). To prevent hydrolysis and evaporation of cocrystallized solvent molecules, the crystals were coated with a

Table 1. Crystallographic Data for the Three Structures

	Nd(tpaam), **6**	La(tpaam), **7**	Lu(tpaam), **8**
formula	$C_{71}H_{110}Cl_9Nd_3N_{14}O_{11}$	$C_{34.25}H_{46.25}I_3LaN_{7.25}O_3$	$C_{36}H_{48.25}I_3LuN_{7.75}O_3$
fw	2087.50	1127.15	1193.24
cryst syst	orthorombic	triclinic	monoclinic
space group	*Pnma*	$P\bar{1}$	*P*2/*n*
a, Å	17.4751(10)	10.1503(5)	24.456(1)
b, Å	28.8954(17)	10.5439(5)	14.1768(6)
c, Å	17.7919(10)	20.3780(9)	26.003(1)
α, Å	90	90.5570(10)	90
β, Å	90	100.4330(10)	101.618(1)
γ, Å	90	92.6060(10)	90
V, Å^3/*Z*	8984.0(9)/4	2142.30(17)/2	8830.6(6)/8
λ	0.710 73	0.710 73	0.710 73
D_{calc}, g cm^{-3}	1.543	1.747	1.791
μ (Mo Kα), mm^{-1}	2.036	3.198	4.374
temp, K	193(2)	143(2)	223(2)
R1, wR2[a]	0.0350, 0.0707	0.0373, 0.0993	0.0371, 0.1029

[a] Structure was refined on F_o^2 using all data: wR2 = $[\sum[w(F_o^2 - F_c^2)^2]/\sum w(F_o^2)^2]^{1/2}$, where $w^{-1} = [\sum(F_o^2) + (aP)^2 + bP]$ and $P = [\max(F_o^2, 0) + 2F_c^2]/3$.

Scheme 1 [a]

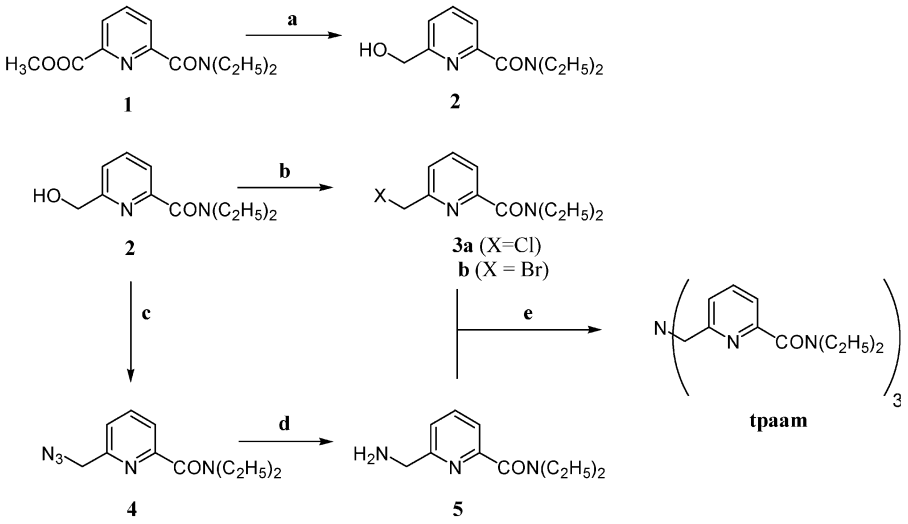

[a] Reagents and conditions: (a) $NaBH_4$, MeOH, reflux (71%); (b) $SOCl_2$, 0 °C (90%) or $SOBr_2$, CH_2Cl_2, 0 °C to room temperature (99%); (c) (1) MsCl, Et_3N, toluene, 0 °C, (2) NaN_3, $^tBu_4NBr$, H_2O/toluene, 90 °C (97%); (d) Pd/C, H_2 (Patm), MeOH, room temperature (93%); (e) K_2CO_3, CH_3CN, reflux (X = Cl, 66%; X = Br, 78%).

light hydrocarbon oil. The cell parameters were obtained with intensities detected on three batches of 15 frames with a 10 s exposure time for Nd and La and a 5 s exposure time for Lu. The crystal−detector distance was 5 cm. For three settings of Φ, 745 narrow data frames for Nd and 1373 narrow data frames for La and Lu were collected for 0.3° increments in *ω* with a 60 s exposure time for Nd and a 30 s exposure time for La and Lu. At the end of data collection, the first 50 frames were recollected to establish that crystal decay had not taken place during the collection. Unique intensities with $I > 10\sigma(I)$ detected on all frames using the Bruker Smart software program[22] were used to refine the values of the cell parameters. The substantial redundancy in data allows empirical absorption corrections to be applied using multiple measurements of equivalent reflections with the SADABS Bruker software program.[22] Space groups were determined from systematic absences, and they were confirmed by the successful solution of the structure (Table 1). Complete information on crystal data and data collection parameters is given in the Supporting Information.

The structures were solved by direct methods using the SHELXTL 5.03 software package,[23] and for all structures, all non-hydrogen atoms were found by difference Fourier syntheses. For complexes **6** and **7**, all non-hydrogen atoms were anisotropically refined on F^2. For all structures, hydrogen atoms were included in calculated positions and refined isotropically. For complex **8**, the carbon and nitrogen atoms of the cocrystallized pyridine molecules were isotropically refined.

3. Results and Discussion

3.1. Synthesis and Characterization of the Ligand tpaam. The synthetic procedure for tris[6-((2-*N*,*N*-diethylcarbamoyl)pyridyl)methyl]amine (tpaam) is summarized in Scheme 1. The starting 6-diethylcarbamoyl-pyridine-2-carboxylic acid methyl ester **1** was prepared from commercially available 2,6-pyridinedicarboxylic acid according to the published procedure of Chauvin et al.[21] Reduction of the ester **1** using sodium borohydride gave the hydroxymethyl derivative **2** in 71% yield. Treatment of the alcohol **2** with pure thionyl chloride or with thionyl bromide in dichloromethane

(22) *SMART*, version 5.1; Bruker; Bruker: Madison, WI, 1995.

(23) Sheldrick, G. M. *SHELXTL*, version 5.03; University of Göttingen: Göttingen, Germany, 1994.

afforded the desired chloromethylated or bromomethylated derivatives **3** in 90% or 99% yield, respectively. The treatment of the alcohol **2** with mesyl chloride and triethylamine in toluene followed by addition of sodium azide, tetrabutylammonium bromide, and water gave the crude azide **4** (yield 97%). This azidomethyl derivative **4** was hydrogenated to afford the amino compound **5** in 93% yield. Finally, condensation of the amino compound **5** with 2-fold molar quantities of the halogenomethyl derivative **3** using potassium carbonate as a base in acetonitrile resulted in the expected tpaam which was purified by reverse phase HPLC chromatography. Note that the use of the bromomethyl derivative **3b** gave tpaam in higher yield (78%).

The ligand tpaam was fully characterized by NMR, ES-MS, and elemental analysis. The ^{1}H NMR spectrum of tpaam in $CDCl_3$ showed eight signals with four signals for the 30 protons of the diethylcarbamoyl groups, one signal for the six protons of the three methylene groups of the pendant arms, and three signals for the nine pyridine protons in agreement with a C_{3v} symmetry of the ligand in solution. The proton NMR spectrum of tpaam in methanol solution also displays a single set of eight signals corresponding to nuclei H^{1-10}, implying C_{3v} symmetry. Proton H^3 could easily be differentiated from H^5 as a strong nuclear Overhauser (NOE) effect is observed between H^3 and H^1 in the {^{1}H ^{1}H} nuclear Overhauser enhancement spectroscopy (NOESY) correlation map.

3.2. Synthesis and Structural Characterization of the Complexes of tpaam. The reaction of $LnCl_3 \cdot H_2O$ (Ln = La, Eu, Nd, Lu) with a stoichiometric amount of tpaam in methanol leads after addition of diethyl ether to the isolation of the complexes [Ln(tpaam)Cl_3] as highly hygroscopic microcrystalline solids. Although the ES-MS spectra and the ^{1}H NMR spectra were in agreement with the presence of species of formula [Ln(tpaam)Cl_3], we were not able to obtain satisfactory elemental analyses. The ^{1}H NMR spectra in deuterated methanol show the presence of only one set of signals in agreement with the presence of undissociated complexes. We obtained crystals suitable for X-ray diffraction for the Nd complex. The crystallographic study revealed the formula $\{[Nd(tpaam)(Cl)(Cl)_{0.5}(MeOH)_{0.5}]_2[Nd(MeOH)(Cl)_5]\}Cl \cdot 3MeOH$, **6**, showing the presence of the dianionic complex $[Nd(MeOH)(Cl)_5]^{2-}$ associated with the cationic complex of tpaam. The ^{1}H NMR spectrum of the mother liquor showed the presence of free ligand which was absent in the starting reaction mixture. The same structure was also obtained when the crystals were prepared from solutions containing a small excess of ligand, whereas we were unable to obtain a crystalline solid in the presence of a large excess of free ligand. The isolation of this unusual product is probably due to its very high insolubility in the crystallization condition and to the higher solubility of the expected [Ln(tpaam)Cl_3] complex. The presence of variable amounts of $LnCl_3$ in the isolated solids and their hygroscopic character are probably responsible for the unsatisfactory elemental analysis of the [Ln(tpaam)Cl_3] complexes.

We obtained satisfactory elemental analyses for the complexes Ln(tpaam)$(ClO_4)_3 \cdot 6H_2O$ (Ln = La, Nd) and for Ln(tpaam)$(OTf)_3$ (Ln = Eu, Tb) which were isolated in 70−80% yield by slow diffusion of diethyl ether into an acetonitrile solution. The proton NMR spectra of these compounds are very similar to those observed for the chloride complexes of tpaam. We failed to obtain crystals of these complexes suitable for X-ray studies.

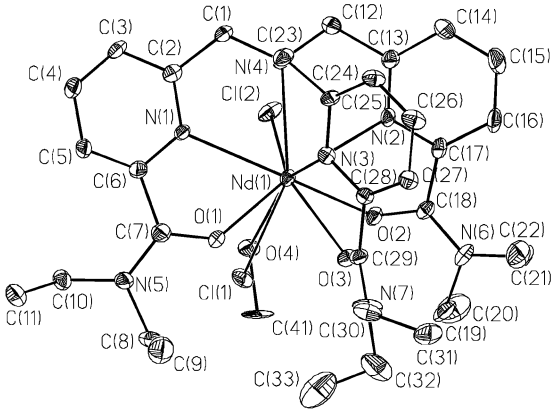

Figure 1. ORTEP diagram of $[Nd(tpaam)(Cl)(Cl)_{0.5}(MeOH)_{0.5}]^{1.5+}$, **6**, with 30% thermal contours for all atoms.

Table 2. Selected Bond Distances (Å) and Angles (deg) in Complex **6**

Nd(1)−O(4)	2.424(3)	N(2)−Nd(1)−N(1)	124.59(6)
Nd(1)−O(3)	2.5070(16)	N(3)−Nd(1)−N(1)	88.62(6)
Nd(1)−O(1)	2.5078(18)	O(4)−Nd(1)−N(4)	142.84(10)
Nd(1)−O(2)	2.5168(16)	O(3)−Nd(1)−N(4)	125.03(5)
Nd(1)−N(2)	2.616(2)	O(1)−Nd(1)−N(4)	109.23(6)
Nd(1)−N(3)	2.6458(19)	O(2)−Nd(1)−N(4)	121.46(6)
Nd(1)−N(1)	2.6554(19)	N(2)−Nd(1)−N(4)	63.76(6)
Nd(1)−N(4)	2.738(2)	N(3)−Nd(1)−N(4)	64.35(6)
Nd(1)−Cl(2)	2.7739(7)	N(1)−Nd(1)−N(4)	60.89(6)
Nd(1)−Cl(1)	2.8516(14)	O(4)−Nd(1)−Cl(2)	74.47(9)
		O(3)−Nd(1)−Cl(2)	147.03(4)
O(4)−Nd(1)−O(3)	92.08(9)	O(1)−Nd(1)−Cl(2)	131.22(4)
O(4)−Nd(1)−O(1)	77.99(9)	O(2)−Nd(1)−Cl(2)	80.50(4)
O(3)−Nd(1)−O(1)	72.12(6)	N(2)−Nd(1)−Cl(2)	79.64(5)
O(4)−Nd(1)−O(2)	71.62(9)	N(3)−Nd(1)−Cl(2)	135.99(5)
O(3)−Nd(1)−O(2)	66.63(5)	N(1)−Nd(1)−Cl(2)	83.46(4)
O(1)−Nd(1)−O(2)	126.81(6)	N(4)−Nd(1)−Cl(2)	74.14(4)
O(4)−Nd(1)−N(2)	128.18(10)	O(4)−Nd(1)−Cl(1)	12.40(9)
O(3)−Nd(1)−N(2)	86.03(6)	O(3)−Nd(1)−Cl(1)	81.98(5)
O(1)−Nd(1)−N(2)	147.20(6)	O(1)−Nd(1)−Cl(1)	68.07(5)
O(2)−Nd(1)−N(2)	60.24(6)	O(2)−Nd(1)−Cl(1)	74.17(5)
O(4)−Nd(1)−N(3)	149.54(10)	N(2)−Nd(1)−Cl(1)	133.88(5)
O(3)−Nd(1)−N(3)	62.33(6)	N(3)−Nd(1)−Cl(1)	137.16(5)
O(1)−Nd(1)−N(3)	78.43(6)	N(1)−Nd(1)−Cl(1)	96.86(5)
O(2)−Nd(1)−N(3)	108.67(6)	N(4)−Nd(1)−Cl(1)	151.70(5)
N(2)−Nd(1)−N(3)	69.71(6)	Cl(2)−Nd(1)−Cl(1)	86.83(3)
O(4)−Nd(1)−N(1)	96.20(10)		
O(3)−Nd(1)−N(1)	128.53(6)		
O(1)−Nd(1)−N(1)	60.37(6)		
O(2)−Nd(1)−N(1)	60.37(6)		

The ORTEP diagram of $[Nd(tpaam)(Cl)(Cl)_{0.5}(MeOH)_{0.5}]^{1.5+}$ is shown in Figure 1, and selected distances and angles are presented in Table 2. The crystals contain two types of nine-coordinate Nd(tpaam) complexes with one complex presenting two bound chloride anions and the other containing one oxygen-bound methanol and one coordinating chloride. In both complexes, the tpaam ligand acts as a heptadentate N4O3 donor. This leads to the presence of a crystallographic disorder resulting in an average crystal structure with half occupancy of the chloride and methanol sites. The geometry of the metal ion can be described as a highly distorted

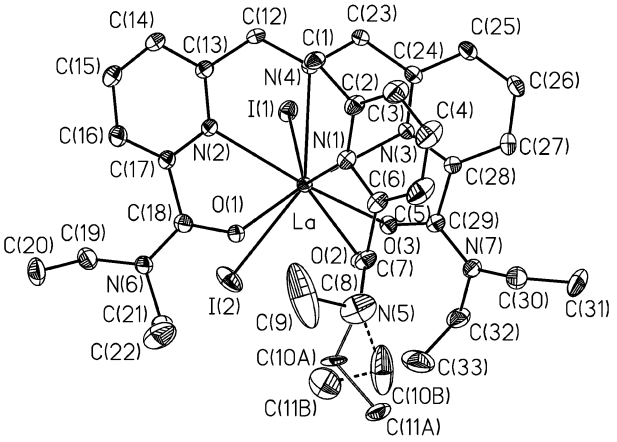

Figure 2. ORTEP diagram of $[La(tpaam)(I)_2]^+$, **7**, with 30% thermal contours for all atoms.

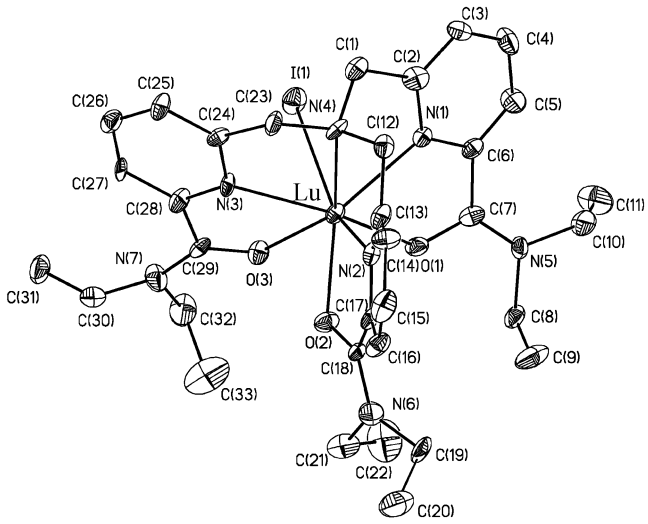

Figure 3. ORTEP diagram of $[Lu(tpaam)(I)]^{2+}$, **8**, with 30% thermal contours for all atoms.

tricapped trigonal prism. Tpaam binds the metal in an asymmetric way with the ligand arms adopting a fanlike configuration. In the counterion $[Nd(MeOH)Cl_5]^{2-}$ the Nd is six-coordinate with an octahedric geometry.

The mean value of the Nd−O_{amide} distances (2.510(5) Å) is in good agreement with the value calculated from the ionic radii[24] (2.513 Å) and is slightly longer than the Nd−$O_{carboxylate}$ distance found in $[Nd(tpaa)]_2$ (2.47(2) Å). The average Nd−$N_{pyridine}$ distance (2.64(2) Å) is also in good agreement with the value expected from the sum of their ionic radii (2.62 Å) and is similar to the one found in the eight-coordinate complex $[Nd(tpa)Cl_3(MeOH)]$ (2.64(5) Å) but is longer than the mean Nd−$N_{pyridine}$ distance found in the dimeric complex $[Nd(tpaa)]_2$ (2.60(3) Å). The Nd−N_{apical} is significantly longer (2.738(2)Å) than the one found in the Nd(tpa) complex (2.668(2) Å).

We were unable to prepare crystals of the other Ln(tpaam)-Cl_3 complexes. In order to obtain crystal structures of different Ln(III) ions to investigate if the ligand tpaam is adapted to bind differently sized lanthanide ions, we decided to use the iodide salts of lanthanides which are soluble in acetonitrile but require handling in anhydrous conditions.

The reaction of $LnI_3(THF)_4$ (Ln = La, Lu) with tpaam in anhydrous acetonitrile/pyridine and addition of *n*-hexane allowed us to isolate crystals of the complexes $[La(tpaam)I_2]I\cdot 0.25py$, **7**, and $[Lu(tpaam)I]I_2\cdot 0.25CH_3CN\cdot 0.5py$, **8**. The Lu complex can be isolated in good yield (80%) from a pyridine solution by adding THF, whereas any attempt to prepare the La complex in larger scale resulted in the formation of oils.

The ORTEP diagram of the cation $[La(tpaam)I_2]^+$ is shown in Figure 2, and the ORTEP diagram of the cation $[Lu(tpaam)I]^{2+}$ is shown in Figure 3; selected distances and angles are given in Tables 3 and 4.

In complex **7** the lanthanum is nine-coordinated by the three amide oxygens, the three pyridyl nitrogens, the capping nitrogen of the tpaam ligand, and two coordinating iodides. The ligand binds the metal in an asymmetric way with the ligand arms adopting a fanlike configuration.

The average La−O_{amide} distance (2.55(6) Å) is very similar to the sum of the ionic radii (2.566 Å) and is only slightly longer than the mean La−$O_{carboxylate}$ distance in the nine-coordinate La(tpaa) (2.50(5) Å). This distance is significantly longer than the La−O_{amide} distance observed in the nine-coordinate lanthanum podate of the nonadentate covalent tripode tris-[2-[2-(6-diethylcarbamoyl-5-yl-pyridin-2-yl)-1-ethyl-1*H*-benzoimidazol-5-yl-methoxyl]ethyl]methane (L1) (2.486(7) Å).[25] The average La−$N_{pyridyl}$ distance (2.70(4) Å) is close to the sum of the ionic radii (2.676 Å) and similar to the mean La−$N_{pyridyl}$ distance in the neutral complex $[La(tpaa)]$ (2.66(5) Å) and to the La−$N_{pyridyl}$ distance in the cationic complex $[LaL1]^{3+}$ (2.695(8) Å). The La−N_{apical} distance (2.862(1) Å) is similar to the one found in nine-coordinate La(tpaa) (2.878(5) Å).

The mean La−O_{amide} distance (2.53(4) Å) found in 10-coordinate $[La(dotam)(OTf)(EtOH)]^{2+}$ is significantly shorter than the sum of the radii (2.62 Å). The shorter values of the La−O_{amide} distance observed for the ligands dotam and L1 are probably due to the higher positive charge of these complexes.

In complex **8** the lutetium is eight-coordinated by the three amide oxygens, the three pyridyl nitrogens, the capping nitrogen of the tpaam ligand, and one coordinating iodide. The ligand tpaam coordinates the metal in a pseudo-C_3 symmetric way with the ligand arms adopting a helical conformation. The disruption of this symmetric arrangement observed in the Nd and La complexes is probably due to the steric hindrance generated by the presence in those complexes of an additional ligand (I, Cl, or MeOH).

The average Lu−O_{amide} distance (2.27(4) Å) is 0.06 Å shorter than the sum of the ionic radii and has the same value for the mean Lu−$O_{carboxylate}$ distance as is found in the monomeric eight-coordinate Lu(tpaa) (2.27(3) Å). The average Lu−$N_{pyridyl}$ distance (2.45(2) Å) is close to the sum of the ionic radii (2.437 Å) and is similar to the mean

(24) Shannon, R. D. *Acta Crystallogr.* **1976**, *A32*, 751.

(25) Koeller, S.; Bernardinelli, G.; Bocquet, B.; Piguet, C. *Chem.—Eur. J.* **2003**, *9*, 1062.

Table 3. Selected Bond Distances (Å) and Angles (deg) in Complex **7**

La−O(2)	2.4801(10)	O(2)−La−N(2)	127.96(4)	O(2)−La−I(2)	93.29(2)
La−O(1)	2.5884(10)	O(1)−La−N(2)	60.13(3)	O(1)−La−I(2)	73.09(2)
La−O(3)	2.5925(9)	O(3)−La−N(2)	163.89(3)	O(3)−La−I(2)	83.03(2)
La−N(3)	2.6616(11)	N(3)−La−N(2)	120.32(3)	N(3)−La−I(2)	140.54(3)
La−N(2)	2.7026(11)	O(2)−La−N(1)	61.28(3)	N(2)−La−I(2)	92.87(3)
La−N(1)	2.7343(12)	O(1)−La−N(1)	73.00(3)	N(1)−La−I(2)	142.41(3)
La−N(4)	2.8625(11)	O(3)−La−N(1)	108.69(3)	N(4)−La−I(2)	144.63(2)
La−I(2)	3.2348(2)	N(3)−La−N(1)	67.82(4)	O(2)−La−I(1)	146.05(2)
La−I(1)	3.31156(19)	N(2)−La−N(1)	84.01(3)	O(1)−La−I(1)	135.44(2)
O(2)−La−O(1)	72.64(3)	O(2)−La−N(4)	120.13(3)	O(3)−La−I(1)	78.07(2)
O(2)−La−O(3)	67.98(3)	O(1)−La−N(4)	104.27(3)	N(3)−La−I(1)	80.43(3)
O(1)−La−O(3)	132.16(3)	O(3)−La−N(4)	118.41(3)	N(2)−La−I(1)	85.93(3)
O(2)−La−N(3)	82.88(3)	N(3)−La−N(4)	61.89(3)	N(1)−La−I(1)	135.26(3)
O(1)−La−N(3)	140.26(3)	N(2)−La−N(4)	58.43(3)	N(4)−La−I(1)	76.63(3)
O(3)−La−N(3)	59.05(3)	N(1)−La−N(4)	61.04(3)	I(2)−La−I(1)	81.468(4)

Table 4. Selected Bond Distances (Å) and Angles (deg) in Complex **8**

Lu1−O(1)	2.220(3)	N3−Lu1−N1	122.92(14)
Lu1−O(2)	2.279(4)	O1−Lu1−N2	98.49(14)
Lu1−O(3)	2.284(4)	O2−Lu1−N2	64.97(13)
Lu1−N(1)	2.433(4)	O3−Lu1−N2	129.72(13)
Lu1−N(2)	2.486(4)	N3−Lu1−N2	96.35(14)
Lu1−N(3)	2.428(4)	N1−Lu1−N2	91.82(14)
Lu1−N(4)	2.576(4)	O1−Lu1−N4	127.29(13)
Lu1−I(1)	3.2282(5)	O2−Lu1−N4	125.79(13)
		O3−Lu1−N4	134.31(13)
		N3−Lu1−N4	68.65(13)
O1−Lu1−O2	79.62(14)	N1−Lu1−N4	64.40(14)
O1−Lu1−O3	95.69(13)	N2−Lu1−N4	65.01(13)
O2−Lu1−O3	70.71(13)	O1−Lu1−I1	95.10(10)
O1−Lu1−N3	162.01(14)	O2−Lu1−I1	141.23(10)
O2−Lu1−N3	97.67(14)	O3−Lu1−I1	71.69(9)
O3−Lu1−N3	66.86(13)	N3−Lu1−I1	75.76(10)
O1−Lu1−N1	66.77(13)	N1−Lu1−I1	72.06(10)
O2−Lu1−N1	135.89(14)	N2−Lu1−I1	152.75(10)
O3−Lu1−N1	137.73(14)	N4−Lu1−I1	87.98(9)

$Lu-N_{pyridyl}$ distance in the neutral complex [Lu(tpaa)] (2.44(3) Å) and is slightly shorter than in the neutral complex [Lu(tpa)Cl_3] (2.51(1) Å). The $Lu-N_{apical}$ (2.597(11) Å) distance is similar to the one found in Lu(tpaa) (2.6071(18) Å) and is slightly longer than the one found in the seven-coordinate [Lu(tpa)Cl_3] complex (2.555(1) Å).

The Ln(III) complexes of tpaam crystallize as monomeric species in the presence of chloride or iodide counterions. Monomeric structures were also found for the chloride complexes of tpa, whereas the lanthanide complexes of tpaa form tetrameric (La), dimeric (Nd−Yb), or monomeric (Lu) structures.

The crystal structures presented here show that the Ln−O and $Ln-N_{pyridyl}$ distances in the complexes of tpaam are similar to those found for the tpaa complexes despite the difference in charge. Whereas it is difficult to comment on the small differences of the $Ln-N_{pyridyl}$ distances between the tpa and tpaam complexes, a significant lengthening of the $Ln-N_{apical}$ distance is found for the tpaam complexes with respect to the tpa ones. In addition, whereas the $Ln-N_{pyridyl}$ distance remains similar in tpa and tpaam complexes going from light to heavy lanthanides, the lengthening of the $Ln-N_{apical}$ distance observed in the tpaam complexes with respect to the tpa complexes is more marked for larger lanthanides.

Although a direct comparison of the metal−ligand distances between the La and Lu complexes is prevented by the different number of coordinated anions, the agreement found in both complexes between the experimental values and the distances calculated from the sum of the ionic radii indicates that the ligand tpaam can encapsulate differently sized Ln(III) ions. However, in the complexes of the larger lanthanides the interaction with the amide oxygens leads to a more important weakening of the interaction with the apical nitrogen (with respect to tpa complexes) than in complexes of the smaller lanthanides.

3.3. Solution Properties. The comparative study of the lanthanide(III) complexes of the two ligands tpaam and tpa allows the evaluation of the effect of pyridine substitution with an amide group on these tripodal structures. The solution behavior of the lanthanide chloride complexes of the tripodes tpaam and tpa was investigated in methanol by proton NMR.

It was previously observed that the proton NMR spectra of [Ln(tpa)Cl_3] are consistent with a 3-fold symmetry of the complex in which all chelating arms of the ligand are equivalent.[18] Proton NMR spectra of the diamagnetic complexes ([La(tpaam)Cl_3] and [Lu(tpaam)Cl_3]) display three signals for the 9 pyridine protons, one signal for the 6 methylene protons, and four signals for the 30 protons of the diethylcarbamoyl groups indicating the presence of C_{3v} symmetric solution species in which all chelating arms of the tpaam ligand are equivalent. The strong intramolecular NOE between protons H^5 and $H^{7,8}$ observed in the NOESY correlation map indicate the anti conformation of the bidentate units in [Ln(tpaam)Cl_3] (i.e., the oxygen atom of the carbonyl group is cis to the nitrogen atom of the pyridine ring) resulting from the presence of metal-bound amide carbonyl groups in methanol solution. Indeed, these NOE effects are not observed in the NOESY correlation map of the free ligand. The lack of NOE effects in the free ligand is compatible with the presence of fast rotation of the diethylcarbamoyl groups on the NMR time scale or with the presence of a rigid syn conformation of the carboxamido-pyridine units. As observed for the diamagnetic podates, the paramagnetic complexes [Ln(tpaam)Cl_3] (Ln = Pr, Nd, Sm, Eu, Tb, Dy, Ho, Er, Tm, Yb) display a C_{3v} symmetrical structure on the NMR time scale. Two-dimensional {^{1}H, ^{1}H} correlation spectroscopy (COSY) NMR spectra allow a reliable assignment of the signals for the Pr, Nd, Sm, Eu, and Yb complexes. For the lanthanide cations in the second part of the 4f series (Ln = Tb, Dy, Ho, Er, Tm), which induce very fast relaxation rates, the proton assignments were done on the basis of the lanthanide-induced shifts. Indeed, further

structural information in solution may be gained from the analysis of the lanthanide-induced shifts. The paramagnetic chemical shift $\delta^{para}_{i,Ln}$ for a proton i and a lanthanide Ln is given by eq 1, where $\delta^{exp}_{i,Ln}$ is the measured chemical shift

$$\delta^{para}_{i,Ln} = \delta^{exp}_{i,Ln} - \delta^{dia}_{i,Ln} = \delta^{c}_{i,Ln} + \delta^{pc}_{i,Ln} \quad (1)$$

and $\delta^{dia}_{i,Ln}$ is the diamagnetic contribution which can be estimated by measuring chemical shifts for isostructural diamagnetic complexes (La or Lu). The term $\delta^{para}_{i,Ln}$ is the sum of contact ($\delta^{c}_{i,Ln}$) and pseudocontact ($\delta^{pc}_{i,Ln}$) shifts. The contact term $\delta^{c}_{i,Ln}$ results from "through-bond" interactions caused by the delocalization of electron spin density. It is ion and nucleus dependent but independent of orientation and can be expressed by eq 2. The term F_i is only dependent

$$\delta^{c}_{i,Ln} = \frac{A_i \langle S_Z \rangle_{Ln}}{\hbar \gamma B_0} = F_i \langle S_Z \rangle_{Ln} \quad (2)$$

on the nucleus i, and $\langle S_Z \rangle_{Ln}$, the spin expectation value of S_Z, depends only on the lanthanide cation. The dipolar or pseudocontact term $\delta^{pc}_{i,Ln}$ results from through-space effects and may be expressed according to eq 3 for axial symmetry,

$$\delta^{pc}_{i,Ln} = \frac{k_{CF}}{T^2}\left(\frac{1 - 3\cos^2\theta_i}{r_i^3}\right) D_{Ln} = G_i k_{CF} D_{Ln} \quad (3)$$

where θ_i and r_i are the polar coordinates relative to the principal magnetic axis for the nucleus i being observed, k_{CF} is the crystal field parameter associated with the complexes, and D_{Ln} is the anisotropic part of the axial magnetic susceptibility tensor. It is generally assumed that the $\langle S_Z \rangle_{Ln}$ and D_{Ln} values are the same for the complexes and the free ion, for which they have been calculated.[26−28] The use of eq 5, which is the linearized form of eq 4,[29] for the proton

$$\delta^{para}_{i,Ln} = F_i \langle S_Z \rangle_{Ln} + G_i k_{CF} D_{Ln} \quad (4)$$

$$\frac{\delta^{para}_{i,Ln}}{\langle S_Z \rangle_{Ln}} = F_i + G_i k_{CF} \frac{D_{Ln}}{\langle S_Z \rangle_{Ln}} \quad (5)$$

paramagnetic chemical shifts in both podates for Pr, Nd, Eu, and Yb produces straight lines indicating the isostructurality of both complex series and allows the prediction of the proton chemical shifts of the lanthanide complexes of the second part of the 4f series. This makes possible the assignment of these nuclei which have very high relaxation rates. Proton chemical shifts of complexes [Ln(tpaam)Cl_3] and [Ln(tpa)Cl_3] are collected in Tables 5 and 6, respectively.

The analysis of the paramagnetic data across the entire rare-earth series for protons in both podates according to eq 5 systematically produces straight lines indicating that no significant structural change occurs across the 4f series for these complexes in methanol solution (Figures 4 and 5). The resulting F_i and G_i terms and agreement factors AF_i and AF_{Ln} are collected in Tables 7 and 8, respectively, for [Ln(tpaam)Cl_3] and [Ln(tpa)Cl_3]. The samarium complexes were not included in the calculation because Sm(III) induces negligible contact and pseudocontact shifts. If H^9 and H^{10}, which display minor lanthanide-induced shifts, are neglected, the agreement factors AF_i (eq 6) are the following: $0.13 < AF_i < 0.33$ for tpaam and $0.07 < AF_i < 0.31$ for tpa. The F_i values

$$AF_i = \sqrt{\frac{\sum_{Ln}(\delta^{exp}_{i,Ln} - \delta^{calc}_{i,Ln})^2}{\sum_{Ln}(\delta^{exp}_{i,Ln})^2}}, \quad AF_{Ln} = \sqrt{\frac{\sum_{i}(\delta^{exp}_{i,Ln} - \delta^{calc}_{i,Ln})^2}{\sum_{i}(\delta^{exp}_{i,Ln})^2}} \quad (6)$$

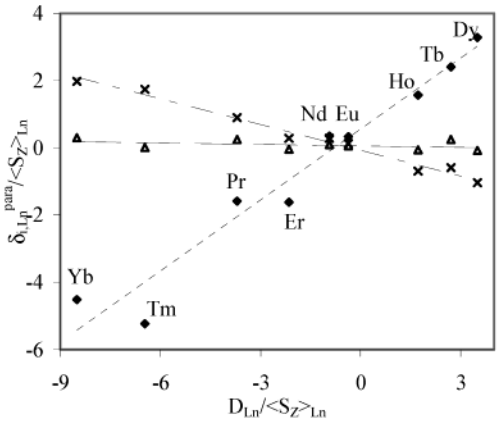

Figure 4. Plots of $\delta^{para}_{i,Ln}/\langle S_Z \rangle_{Ln}$ vs $D_{Ln}/\langle S_Z \rangle_{Ln}$ for protons H^1 (◆), H^4 (△), and H^7 (×) in [Ln(tpaam)Cl_3] in CD_3OD at 298 K.

Table 5. NMR Shifts (in ppm, with Respect to TMS) for the Complexes [Ln(tpaam)Cl_3] in CD_3OD at 298 K

	H^1	H^3	H^4	H^5	H^7	H^8	H^9	H^{10}
tpaam	3.92	7.70	7.87	7.40	3.31	1.14	3.56	1.27
[La(tpaam)Cl_3]	4.42	7.68	8.10	7.80	3.72	1.36	3.77	1.42
[Pr(tpaam)Cl_3]	−0.28	6.25	8.85	10.90	6.38	2.85	5.63	2.56
[Nd(tpaam)Cl_3]	6.01	7.75	8.52	9.33	4.96	2.02	5.67	2.56
[Sm(tpaam)Cl_3]	4.64	7.46	7.88	7.61	3.83	1.43	4.16	1.69
[Eu(tpaam)Cl_3]	0.82	6.89	7.47	5.69	2.42	0.87	2.01	0.20
[Tb(tpaam)Cl_3]	−72.2	−22.8	0.4	17.2	22.7	8.6	9.7	8.6
[Dy(tpaam)Cl_3]	−89.0	−19.4	10.3	39.6	33.2	17.3	10.3	4.8
[Ho(tpaam)Cl_3]	−31.2	−3.0	9.5	23.6	19.5	9.8	12.8	5.1
[Er(tpaam)Cl_3]	29.1	15.5	8.6	4.0	−0.7	0.1	9.9	2.5
[Tm(tpaam)Cl_3]	47.4	21.1	8.1	−3.5	−10.6	−4.2	5.9	0.3
[Yb(tpaam)Cl_3]	16.08	11.24	7.34	2.91	−1.42	−1.29	1.91	0.4
[Lu(tpaam)Cl_3]	4.65	7.81	8.21	7.94	3.80	1.37	3.86	1.50

Table 6. NMR Shifts (in ppm, with Respect to TMS) for the Complexes [Ln(tpa)Cl_3] in CD_3OD at 298 K

	H^1	H^3	H^4	H^5	H^6
tpa	3.93	7.74	7.88	7.39	8.52
[La(tpa)Cl_3]	4.53	7.41	7.81	7.34	9.1
[Pr(tpa)Cl_3]	11.92	8.93	7.34	4.85	−2.43
[Nd(tpa)Cl_3]	10.25	9.12	8.07	6.95	5.77
[Eu(tpa)Cl_3]	−3.67	4.80	7.51	7.04	10.91
[Tb(tpa)Cl_3]	77	19	−2.8	−26.9	−121
[Dy(tpa)Cl_3]	56	17	−2.2	−25.9	−130
[Ho(tpa)Cl_3]	33	12.7	3.1	−8.8	−55
[Er(tpa)Cl_3]	−11	0.7	7.8	11.4	31
[Yb(tpa)Cl_3]	−4	3.99	8.53	12.12	31.6
[Lu(tpa)Cl_3]	4.58	7.49	7.92	7.45	9.18

(26) Golding, R. M.; Halton, M. P. *Aust. J. Chem.* **1972**, *25*, 2577.
(27) Bleany, B.; Dobson, C. M.; Levine, B. A.; Martin, R. B.; Williams, R. J. P.; Xavier, A. V. *J. Chem. Soc., Chem. Commun.* **1972**, 791.
(28) Bleany, B. *J. Magn. Reson.* **1972**, *8*, 91.
(29) Reilly, C. N.; Good, B. W.; Desreux, J. F. *Anal. Chem.* **1975**, *47*, 2110.

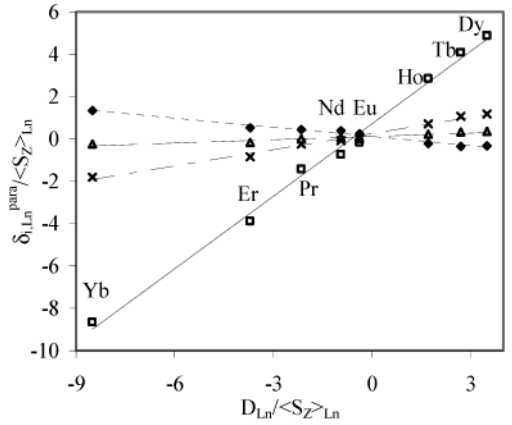

Figure 5. Plots of $\delta_{i,Ln}^{para}/\langle S_Z\rangle_{Ln}$ vs $D_{Ln}/\langle S_Z\rangle_{Ln}$ for protons H^3 (◆), H^4 (△), H^5 (×), and H^6 (□) in [Ln(tpa)Cl_3] in CD_3OD at 298 K.

Table 7. Computed Values for Contact (F_i) and Pseudocontact ($G_i' = G_i \times k_{CF}$) Terms for Proton Nuclei in Paramagnetic Complexes [Ln(tpaam)Cl_3] in CD_3OD at 298 K

	H^1	H^3	H^4	H^5	H^7	H^8
F_i	0.5(2)	0.18(8)	0.06(5)	−0.03(9)	−0.07(5)	−0.05(4)
G_i'	0.70(6)	0.22(2)	−0.02(1)	−0.23(2)	−0.26(1)	−0.12(1)
AF_i	0.13	0.18	0.33	0.30	0.17	0.28

	Ln								
	Pr	Nd	Eu	Tb	Dy	Ho	Er	Tm	Yb
AF_{Ln}	0.10	0.13	0.17	0.20	0.11	0.20	0.34	0.20	0.12

Table 8. Computed Values for Contact (F_i) and Pseudocontact ($G_i' = G_i \times k_{CF}$) Terms for Proton Nuclei in Paramagnetic Complexes [Ln(tpa)Cl_3] in CD_3OD at 298 K

	H^1	H^3	H^4	H^5	H^6
F_i	0.0(3)	0.11(4)	0.13(2)	0.25(4)	0.72(1)
G_i'	−0.49(7)	−0.14(1)	0.05(5)	0.26(1)	1.14(4)
AF_i	0.31	0.13	0.14	0.11	0.07

	Ln							
	Pr	Nd	Eu	Tb	Dy	Ho	Er	Yb
AF_{Ln}	0.14	0.23	0.52	0.21	0.04	0.14	0.14	0.12

calculated for protons having a very high pseudocontact term, G_i, are not accurate because the D_{Ln} values used in the calculation are taken as those of the free ion. The contact terms of the H^1 and H^6 nuclei that are very close to the paramagnetic center are thus not discussed. In the [Ln(tpa)Cl_3] podates, the sizable F_i values ($0.11 < F_i < 0.25$) of the aromatic protons H^{3-5} demonstrate a significant spin delocalization onto the coordinated pyridine ring, which is higher than that observed in podates with ligands bearing three tridente coordination units, pyridine-2,6-dicarboxamide.[17] However, in the [Ln(tpaam)Cl_3] complexes, F_i values are very small even for the aromatic protons ($-0.03 < F_i < 0.18$), and the spin delocalization onto the coordinated pyridine ring is thus smaller than in [Ln(tpa)Cl_3]. This observation could be interpreted as the result of a weaker $Ln-N_{pyridine}$ interaction in the tpaam complexes with respect to the tpa complexes.

It has been shown that concomitant variations of the second-order crystal field parameter k_{CF} can mask structural changes occurring near the middle of the lanthanide series.[30] Equation 7, proposed by Geraldes et al.,[31] does not depend

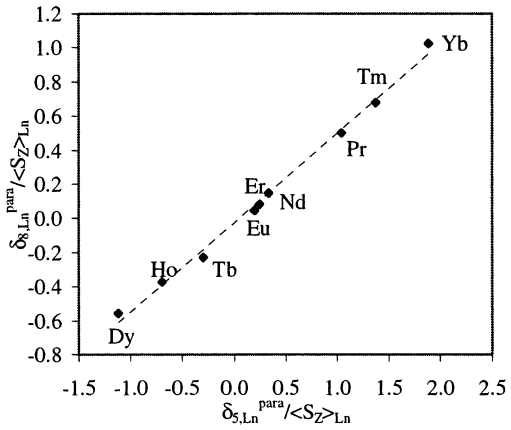

Figure 6. Plots of $\delta_{i,Ln}^{para}/\langle S_Z\rangle_{Ln}$ vs $\delta_{k,Ln}^{para}/\langle S_Z\rangle_{Ln}$ for the H^5, H^8 pair in [Ln(tpaam)Cl_3] in CD_3OD at 298 K.

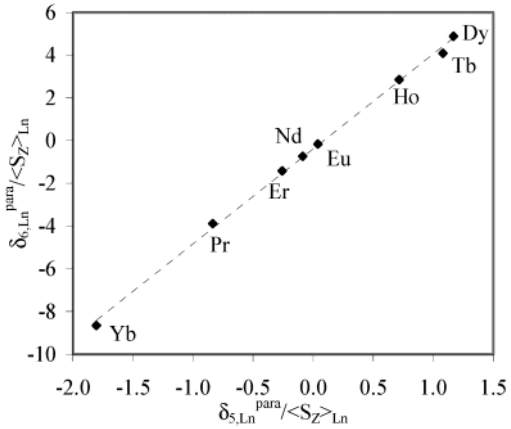

Figure 7. Plots of $\delta_{i,Ln}^{para}/\langle S_Z\rangle_{Ln}$ vs $\delta_{k,Ln}^{para}/\langle S_Z\rangle_{Ln}$ for the H^5, H^6 pair in [Ln(tpa)Cl_3] in CD_3OD at 298 K.

on crystal field parameters, and any deviation from linearity in $\delta_{i,Ln}/\langle S_Z\rangle_{Ln}$ versus $\delta_{k,Ln}/\langle S_Z\rangle_{Ln}$ plots along the lanthanide series can safely be ascribed to structural changes. The

$$\frac{\delta_{i,Ln}^{para}}{\langle S_Z\rangle_{Ln}} = \left(F_i - F_k\frac{G_i}{G_k}\right) + \frac{G_i}{G_k}\frac{\delta_{k,Ln}^{para}}{\langle S_Z\rangle_{Ln}} \qquad (7)$$

analysis of the paramagnetic chemical shifts, for [Ln(tpa)Cl_3] and [Ln(tpaam)Cl_3] podates, with the two-nuclei crystal-field independent method according to eq 7 gives straight lines (see Figures 6 and 7) confirming that no structural change occurs in methanol solution for these complexes, although different structures are observed in the solid state for lanthanum and lutetium cations. Some pairs of protons give moderate correlation coefficients, suggesting a rather flexible arrangement of the tripodal ligand in the complexes which slightly varies with the size of the metal ion.

An insight into the structure of the paramagnetic complexes in solution may also be gained by the lanthanide-induced relaxation (LIR). The inner sphere relaxation rates may have contributions from the contact, dipolar, and Curie mechanisms. The relative importance of the various relax-

(30) Ouali, N.; Bocquet, B.; Rigault, S.; Morgantini, P.-Y.; Weber, J.; Piguet, C. *Inorg. Chem.* **2002**, *41*, 1436.
(31) Platas, C.; Avecilla, F.; de Blas, A.; Geraldes, C. F. G. C.; Rodriguez-Blas, T.; Adams, T.; Mahia, J. *Inorg. Chem.* **1999**, *38*, 3190.

ation mechanisms has been analyzed in detail.[32] For protons the contact contribution to the lanthanide-induced relaxation rates is negligible compared to the dipolar terms. Both dipolar relaxation rate enhancement contributions have the same dependence on the distance r_i between the nucleus H_i and the Ln(III) cation: the paramagnetic longitudinal relaxation time of a proton H^i is thus proportional to the sixth power of the lanthanide−proton distance r_i in solution (eq 8).[33]

$$\frac{1}{T_1^{i,\text{para}}} = \frac{1}{T_1^{i,\text{exp}}} - \frac{1}{T_1^{i,\text{dia}}} = \frac{A}{r_i^6} \tag{8}$$

The proton longitudinal relaxation rates have been measured at 400 MHz and 298 K for both series of podates. The paramagnetic contributions to these rates ($1/T_1^{i,\text{para}}$) are then obtained by subtraction of the diamagnetic term ($1/T_1^{i,\text{dia}}$), which is estimated from the proton longitudinal relaxation rate in the corresponding lanthanum complex (eq 7). These measurements confirm the assignment of the two ethyl groups of the amides in [Ln(tpaam)Cl_3]. Although the proton longitudinal relaxation times of nuclei H^{7-10} are averaged by the rotation of the C−N bond of the amide, the paramagnetic relaxation times of H^7 and H^8 are always much longer than those of H^9 and H^{10}, which are cis to the carbonyl group and thus closer to the paramagnetic center. Among the three aromatic protons H^{3-5}, H^4 is the most distant from the lanthanide cation and has indeed the longest T_1, whereas nuclei H^3 and H^5 display very similar relaxation rates. In the [Ln(tpa)Cl_3] complexes, the aromatic proton H^6, which is ortho to the pyridine nitrogen atom and thus very close to the paramagnetic center, displays the fastest relaxation rate.

Precise information about the location of the lanthanide cation in the ligand cavity may be obtained from the H^3 and H^5 relaxation rates. The Ln−proton distances r_i have been calculated for the aromatic protons from the paramagnetic relaxation times in methanol with eq 9, where r_{ref} is a reference distance taken as the average Ln−H^4 distance in the crystallographic structures of the neodymium complexes (Tables 9 and 10).[34] In the [Ln(tpa)Cl_3] complexes (Ln = Pr−Er), the longitudinal relaxation time measured for H^5 is greater than for H^3, demonstrating that H^5 is more distant from the metal center than H^3 (Table 10). In the [Ln(tpaam)-Cl_3] podates (Ln = Pr−Ho), a reverse effect is observed: in solution, H^3 is more distant from the metal center than H^5 (Table 9). These distances evaluated in methanol solution show the same trends as the values found in the solid-state structure of the Nd(III) complexes, although the difference between r_3 and r_5 is larger in solution. They are also in agreement with the solid-state distance between the Nd(III) cation and the apical nitrogen of the ligand, 2.668(2) and 2.738(2) Å in the tpa[18] and the tpaam complexes, respectively, indicating that in the tpaam ligand the cation moves slightly away from the apical nitrogen as a result of the presence of the additional binding carbonyl groups. At the end of the lanthanide series (Ln = Er−Yb for [Ln(tpaam)-Cl_3] and Ln = Yb for [Ln(tpa)Cl_3]), the distances r_3 and r_5 tend to have the same values, indicating that the metal is located at the same distance from these two protons for the smallest lanthanide ions. This is in agreement with the rather similar $Lu-N_{\text{apical}}$ distances observed in the solid-state structures of the Lu(tpaam) (2.597(11) Å) and of the Lu(tpa) (2.555(1) Å) complexes. These results suggest that the functionalization of the tpa ligand with carbamoyl groups induces some steric constraints which are more pronounced for the larger cations. Indeed the optimization of the Ln−O interaction in the tpaam complexes requires a weakening of the $Ln-N_{\text{apical}}$ bond. This effect is larger for the larger ions.

$$r_i = r_{\text{ref}}\left(\frac{T_1^{i,\text{para}}}{T_1^{\text{ref,para}}}\right)^{1/6} \tag{9}$$

Table 9. Estimated Ln−H^i Distances in Å for [Ln(tpaam)Cl_3] in CD_3OD at 298 K from T_1 Measurements and Eq 8

Ln	H^3	H^4 (ref)	H^5
Pr	5.49	6.29	5.35
Nd	5.55	6.29	5.36
Eu	5.49	6.29	5.35
Tb	5.61	6.29	5.35
Ho	5.44	6.29	5.17
Er	5.49	6.29	5.50
Tm	5.47	6.29	5.48
Yb	5.47	6.29	5.49
Nd (solid)[a]	5.53	6.29	5.49

[a] Averaged proton−lanthanide distances over the three distances measured in the solid-state structure of $[Nd(tpaam)Cl_{1.5}(CH_3OH)_{0.5}]^{1.5+}$.

Table 10. Estimated Ln−H^i Distances in Å for [Ln(tpa)Cl_3] in CD_3OD at 298 K from T_1 Measurements and Eq 8

Ln	H^3	H^4 (ref)	H^5	H^6
Pr	5.28	6.29		3.32
Nd	5.27	6.29	5.57	3.42
Eu		6.29	5.54	3.36
Tb	5.40	6.29	5.66	3.56
Dy	5.36	6.29	5.53	
Ho	5.46	6.29	5.60	3.47
Er	5.39	6.29	5.50	3.59
Yb	5.48	6.29	5.46	3.39
Nd (solid)[a]	5.50	6.29	5.64	3.47

[a] Averaged proton−lanthanide distances over the three distances measured in the solid-state structure of [Nd(tpa)Cl_3(CH_3OH)].[18]

The differences observed between the distances found in solution and in the solid state may also arise from differences in counterion coordination. The values of the conductivities measured on 10^{-3} mol L^{-1} methanol solutions of [Ln(tpaam)-Cl_3] indicate the presence of a 2:1 electrolyte[35] (Λ_M = 186 (La) and 230 S cm^2 mol^{-1} (Lu)). Therefore, only one chloride counterion is coordinated to the lanthanide cation in methanol solution, whereas the solid-state structure of the Nd complex shows the presence of 1.5 coordinated chlorides (resulting from the presence in the crystal of species containing one coordinated chloride and species containing two coordinated chlorides). Methanol solutions of 10^{-3} mol L^{-1} [Ln(tpa)-Cl_3] indicate the coexistence of 1:1 and 1:2 electrolytes (Λ_M

(32) Peters, J. A.; Huskens, J.; Raber, D. J. *Prog. Nucl. Magn. Reson. Spectrosc.* **1996**, *28*, 283.
(33) Kemple, M. D.; Ray, B. D.; Lipkowitz, K. B.; Prendergast, F. G.; Rao, B. D. N. *J. Am. Chem. Soc.* **1988**, *110*, 8275.
(34) Renaud, F.; Piguet, C.; Bernardinelli, G.; Bünzli, J.-C. G.; Hopfgartner, G. *Chem.—Eur. J.* **1997**, *3*, 1646.
(35) Geary, W. J. *Coord. Chem. Rev.* **1971**, *7*, 81.

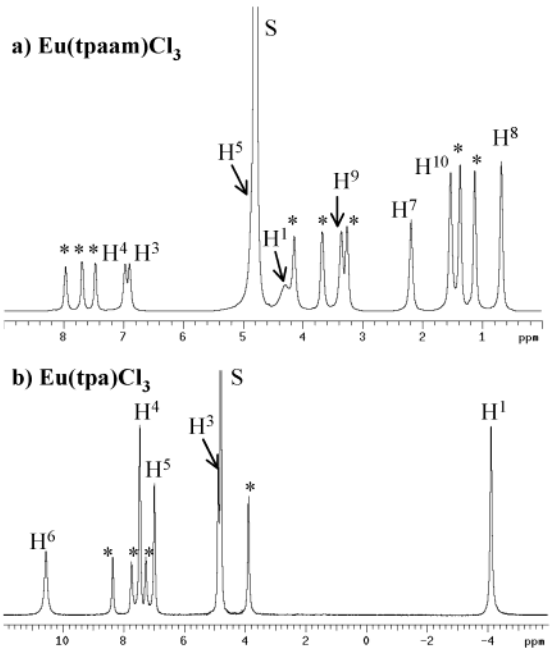

Figure 8. 400 MHz NMR spectra at 298 K of 0.01 mol L^{-1} solutions in D_2O of (a) Eu(tpaam)Cl_3 and (b) Eu(tpa)Cl_3. (∗ = free ligand).

= 128 (La) and 145 S cm^2 mol^{-1} (Lu)), pointing to the coordination of one or two chloride anions to the lanthanide, whereas the three chloride ions are associated with the 4f cation in the solid-state structures.

Proton NMR spectra at 298 K of [Ln(tpaam)Cl_3] complexes in D_2O show a partial dissociation of the tpaam ligand with distinct signals for the complexed and the free form of the ligand. The complexed ligand displays three signals for the 9 pyridine protons, one signal for the 6 methylene protons, and four signals for the 30 protons of the diethylcarbamoyl groups indicating the presence of C_{3v} symmetric solution species. The dissociation of Eu(tpa)Cl_3 and Eu(tpaam)Cl_3 in water is shown in the proton NMR spectra of Figure 8, where the signals have been assigned by NOESY. The formation constant of the Eu(tpaam)Cl_3 complex in D_2O at 298 K was determined by integration of the ^1H NMR signals corresponding to the complex and to the free tpaam ($\log(\beta_{110}) = 2.34(4)$). This value is very similar to the value previously reported for tpa ($\log(\beta_{110}) = 2.49(4)$ at 298 K). Finally, the addition of amide groups to the ligand tpa does not lead to any increase in stability of the lanthanide complexes of tpaam with respect to tpa, even though the amide groups are coordinated to the metal, as demonstrated by the NOE effect between H^5 and H^7 observed in the NOESY spectra of the podate in water.

4. Conclusions

The structural studies described here show that the three amide carbonyl oxygen atoms of the ligand tpaam are coordinated to the lanthanide(III) ions both in the solid state and in methanol solution. From the available structural data it is difficult to draw a conclusion concerning the different strengths of the $Ln-N_{pyridine}$ interactions in the tpaam complexes and in the tpa complexes. Conversely, the values of the $Ln-N_{apical}$ distances in the reported crystal structures and the structural studies in solution point to a weaker $Ln-N_{apical}$ interaction in the tpaam compounds than in the tpa complexes. The tpaam ligand coordinates the Ln(III) ions strongly with the three amide oxygens, with Ln−O bond distances similar to the ones found for the triscarboxylate ligand tpaa.

The contribution of amide functional groups to the stability of lanthanide complexes is important in dota and dtpa derivatives. Quite surprisingly, the addition of three coordinating amide oxygens to the tripodal ligand tpa did not result in an increase of the stability of the cationic lanthanide complexes of tpaam toward ligand dissociation in water. One possible interpretation of these results could be that the amide carbonyl oxygens are not tightly bound to the metal in solution and they are easily displaced by water molecules. However, the proton NMR studies show that the amide groups are coordinated to the metal on the NMR time scale in solution.

The unexpectedly similar stability found for the tpa and tpaam Ln(III) complexes is more likely the result of a lower contribution to stability of the metal−nitrogen interactions associated with an unfavorable desolvation enthalpy caused by the increased number of water molecules displaced by the heptadentate ligand with respect to tetradentate tpa. The lowered metal−nitrogen interactions in the ligand tpaam probably arise from the electron-withdrawing effect of the amide groups decreasing the σ-donor character of the pyridine nitrogen atoms and from the steric interactions weakening the $Ln-N_{apical}$ bond.

Furthermore, the pyridine nitrogen is a weaker donor than tertiary amine donors as found in dota derivatives and therefore yields complexes with a larger residual positive charge. This may result in a higher affinity for water molecules with respect to the dota systems that would then make more difficult their exchange with the carboxamide groups.

These results provide significant information for future ligand design of cationic lanthanide complexes active in catalyzing RNA cleavage in vivo. Detailed studies of the structure and of the thermodynamic quantities in water are in progress in order to further investigate the different parameters leading to the similar stability of tpaam and tpa complexes toward ligand dissociation in water.

Acknowledgment. This work was supported by the Commissariat à l'Energie Atomique, Direction de l'Energie Nucléaire. We thank Colette Lebrun for recording the mass spectra.

Supporting Information Available: Tables of experimental longitudinal relaxation times of protons in the [Ln(tpaam)Cl_3] and [Ln(tpa)Cl_3] complexes; complete tables of crystal data and structure refinement, atomic coordinates, bond lengths and angles, anisotropic displacement parameters, and hydrogen coordinates for complexes **6**−**8**; X-ray crystallographic data in CIF format. This material is available free of charge via the Internet at http://pubs.acs.org.

IC034692E